UNBIASED NOISE ESTIMATION AND DENOISING IN PARALLEL MAGNETIC RESONANCE IMAGING

Pasquale Borrelli

University of Naples Federico II
Dept. of Advanced Biomedical Sciences
Via Pansini 5, 80131 Naples, Italy

Giuseppe Palma, Marco Comerci, Bruno Alfano

National Research Council of Italy
Inst. of Biostructures and Bioimaging
Via De Amicis 95, 80145 Naples, Italy

ABSTRACT

In magnetic resonance (MR) clinical practice, noise estimation is usually performed on Rayleigh-distributed background (no signal area) of magnitude images. Although noise variance in quadrature MR images is considered spatially independent, parallel MRI (pMRI) techniques as SENSE or GRAPPA generate spatially varying noise (SVN) distribution. In this scenario noise estimation from background may produce biased results. To address these limitations we introduce a novel noise estimation scheme based on local statistics. Our method turns out to be more accurate than the other pMRI noise estimation schemes previously described in the literature. Denoising performances, measured by visual inspection and peak signal-to-noise ratio (PSNR), of Non-Local Means denoising filters (NLM) are considerably improved using SVN-NLM in case of inhomogeneous noise. Furthermore, SVN-NLM behaves as well as standard NLM when homogeneous noise was added, thus proving to be a robust and powerful denoising algorithm for arbitrary MRI datasets.

Index Terms— Noise estimation, denoising, parallel MRI, non-local means, Rician noise

1. INTRODUCTION

Noise estimation and, consequently, denoising are crucial steps in most post-processing tasks of MRI and, particularly, of MR image quantitation. In standard quadrature MRI (hereafter, sMRI), both real and imaginary images show an uncorrelated Gaussian noise whose variance is uniform all over the field of view (FOV). Once the magnitude of the complex images is extracted, the resulting noise follows a Rician distribution, whose variance can be accurately estimated from the variance of the voxel values (Rayleigh-distributed) in the image background (*i.e.* the no-signal area) [1, 2].

However, as soon as images show a spatially varying noise distribution, such background-based noise estimation schemes produce biased results [3, 4].

This work was partially funded by FIRB-MERIT RBNE08E8CZ and DSB-CNR/MIUR "Aging" project.

Parallel MRI is an emerged technique that increases the image acquisition rate by sampling a reduced amount of k-space data with an array of receiving coils [5, 6]. Generalized auto-calibrating partially parallel acquisition (GRAPPA) and sensitivity-encoded (SENSE) MRI are most common image reconstruction schemes in pMRI. Both reconstruction algorithms share the incorporation of coil-sensitivity profiles into the image reconstruction process [7]. In GRAPPA algorithm missing k-space lines are computed before full-image is reconstructed for each receiver channel [8]. On the other hand, SENSE algorithm reconstructs complex image for each receiver channel and then final images are pixel-wise multiplied by appropriate coil sensitivity mask [9]. The application of multi-surface coil arrays and reconstruction filter can influence the statistical distribution of image noise [10]. In this scenario, variance of background regions will lead to innacurate estimations of the true local noise if a uniform Rayleigh distribution is erroneously assumed [4].

In the context of denoising algorithms, one of the most performing and robust denoising approaches is the non-local means (NLM) filter, introduced in [11]. NLM filter assumes that the restoring function for a given point is a mean of all the image values, largely weighted according to the radiometric similarity between voxels and only weakly tied to a spatial proximity criterion. In particular, it has been shown that NLM filter guarantees the homogeneity of flat zones, preserves edges and fine structures, and transforms white noise into white noise, thus avoiding the introduction of artifacts and spurious correlated signal [11, 12]. Although there are some algorithm variants that take into account spatially varying noise distribution in image to be filtered [13, 14, 15], at the best of our knowledge, a robust and accurate noise estimation in a NLM pipeline has been poorly investigated.

In this paper we present a novel noise estimation based on NLM filter and local statistics. Our local mask does not need an *a priori* knowledge of sensitivity maps, subsampling factor and geometry factor. Therefore, our noise estimation technique is successfully applicable to MR images with both spatially varying and uniform noise distribution.

The plan of the paper is as follows. In §2 we briefly review

978-1-4799-2893-4/14/$31.00 ©2014 IEEE

the noise properties of standard (§2.1) and parallel (§2.2) MR images. To follow, in §3 we present the details of NLM denoising scheme (§3.1) we used to extract the local noise mask (§3.2) and to produce the actual restored images. Finally, in §4 and §5 we present and discuss the results, comparing the accuracy of our algorithm with the ones already described in literature.

2. THEORY

2.1. Spatially independent noise in sMRI

The full k-space acquired in sMRI is assumed to be corrupted with Gaussian white noise. After Fourier transform, real and imaginary images are still corrupted by uncorrelated Gaussian noise with same variance in both complex components. The non-linear transformation leading to magnitude images modifies the noise distribution, which shows a Rician probability density function (PDF):

$$p_M(M|A,\sigma) = \frac{M}{\sigma^2} e^{-\frac{M^2+A^2}{2\sigma^2}} I_o \frac{AM}{\sigma^2} \epsilon(M), \tag{1}$$

where σ^2 is the noise variance in real and imaginary images; A is the noise-free image; M is the actual magnitude image; I_o is the 0^{th} order modified Bessel function of first kind and ϵ is the Heaviside function. In case of high SNR, the Rician distribution tends to the Gaussian one, while, in the opposite limit ($A = 0$), it becomes the Rayleigh distribution:

$$p_M(M|\sigma) = \frac{M}{\sigma^2} e^{-\frac{M^2}{\sigma^2}}. \tag{2}$$

To avoid wrap-around artifacts, MR images are usually acquired with pretty large background area, so that the noise amplitude can be easily evaluated on no-signal image segment. Given the standard deviation $\hat{\sigma}$ of the image background, σ of Eqs. 1 and 2 is computed according to [1]:

$$\sigma^2 = (2 - \frac{\pi}{2})\hat{\sigma}^2. \tag{3}$$

2.2. Noise from parallel MR images

In pMRI raw data represent the subsampled k-spaces acquired from a multiple-coil system.

In case of GRAPPA technique, [16] shows that in a good approximation the magnitude image PDF is a non-central χ distribution, as if noise were distributed identically and independently in each coil:

$$p_{M_L}(M_L|A_L,\sigma_n,L) = \frac{A_L^{1-L}}{\sigma_n^2} M_L^L e^{-\frac{M_L^2+A_L^2}{2\sigma_n^2}} I_{L-1}\frac{A_L M_L}{\sigma_n^2}\epsilon(M_L), \tag{4}$$

where L is the number of coils, M_L and A_L are respectively magnitude image and noise-free image reconstructed with sum-of-squares method and I_L is L^{th} order Bessel function of first kind.

On the other hand, SENSE reconstructs sub-sampled acquisitions in the spatial domain, noise distribution follows a non-stationary Rician PDF [17] whose variance is:

$$\sigma_s^2 = r\sigma^2 |W_i|^2, \tag{5}$$

where σ^2 is noise variance without subsampling, r is the reduction factor and W_i is the reconstruction matrix depending on sensitivity map for each coil.

3. MATERIALS AND METHODS

3.1. Non-local means denoising filter

An N-D image X can be considered as a real function $X : \mathbb{R}^N \to \mathbb{R}$ with a bounded support $\Omega \subset \mathbb{R}^N$. The NLM filter [11] is a class of endomorphisms of the image space, identified by 2 parameters (a and h), that acts as follows:

$$[\text{NLM}_{a,h}(X)](\vec{x}) = Y(\vec{x}) = \frac{\int_\Omega \exp\left[-\frac{d_a^2(\vec{x},\vec{y})}{h^2}\right] X(\vec{y})d\vec{y}}{\int_\Omega \exp\left[-\frac{d_a^2(\vec{x},\vec{y})}{h^2}\right] d\vec{y}}, \tag{6}$$

where

$$d_a^2(\vec{x},\vec{y}) \equiv \int_{\mathbb{R}^N} \left|X(\vec{x}+\vec{t}) - X(\vec{y}+\vec{t})\right|^2 \cdot \frac{\exp -\frac{\|\vec{t}\|^2}{2a^2}}{(2\pi)^{n/2}\cdot a} d\vec{t}. \tag{7}$$

Therefore, given a search radius M, for each voxel i located at $\vec{x}_i$ we define a search box V_i as

$$V_i \equiv \left\{ \vec{x}_j \in \Omega \,\middle|\, \|\vec{x}_j - \vec{x_i}\|_\infty < M \right\}. \tag{8}$$

Analogously, given a similarity radius $d \sim a$, for each voxel $\vec{x}_j$ within a given search box V_i, we can define a similarity box

$${}_jB_i \equiv \left\{ \vec{x}_k \in \Omega \,\middle|\, \|\vec{x}_k - \vec{x_j}\|_\infty < d \right\}. \tag{9}$$

If the image is defined on a discrete grid, a suitable filter implementation is:

$$Y_i = \frac{\sum_{\vec{x}_j \in V_i} \exp\left[-\frac{\|{}_jB_i - {}_iB_i\|_2^2}{h^2}\right] X_j}{\sum_{\vec{x}_j \in V_i} \exp\left[-\frac{\|{}_jB_i - {}_iB_i\|_2^2}{h^2}\right]}, \tag{10}$$

The filter strength, which is determined by h, can be automatically tuned to obtain an optimized denoising, independently from the search radius M and the standard deviation of noise σ:

$$h^2 = 2\beta\sigma^2 |V_i| \tag{11}$$

($\beta \sim 1$ is an adimensional constant to be manually tuned).

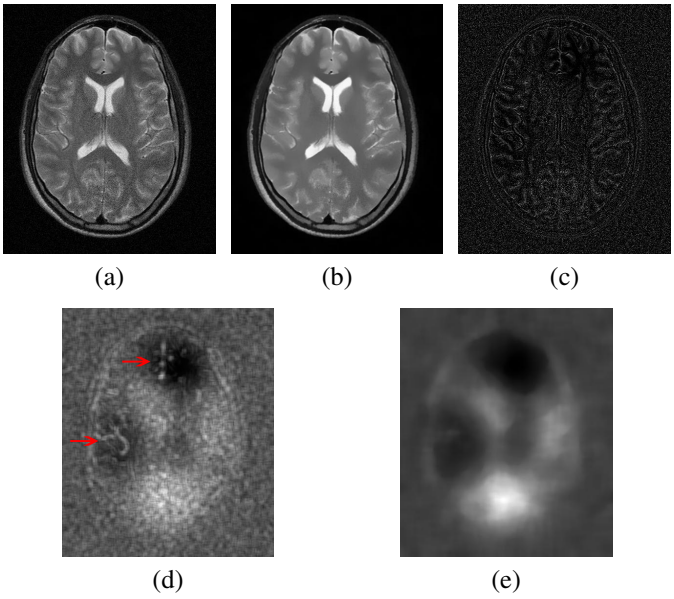

Fig. 1. Spatially varying noise estimation steps in our method. Difference image (c) between noisy image (a) and NLM filtered image (b) was used to estimate local variances (d). Definitive noise mask (e) was obtained by applying a median filter to remove patch-related effects and residual signal structures (see the red arrows) from (d).

3.2. Estimation of local variances

To handle potential inhomogeneities of noise power within the general context of MRI, we considered a local approach to estimate a mask of noise amplitude of input noisy image.

First, we extracted an only-noise image (Fig. 1(c)) as difference between input image (Fig. 1(a)) and the image denoised with a standard NLM algorithm (Fig. 1(b)): we set a pretty high filter streght ($\beta = 1.5$) in order to extract the noise as much as possible, still preserving the edges of the image structures from an excessive blurring. Then, we calculated a patch-based second order central moment of the only-noise image (Fig. 1(d)). To avoid patch-related effects and to wash out the spurious hyper-intensities (red arrows) in Fig. 1(d) around the image edges due to the unavoidable structure blurring introduced by NLM filter, we applied a median filter (which is particularly effective in removing low-cardinality structures – pointed out by the red arrows in the figure) to obtain the final mask of local variances (Fig. 1(e)).

3.3. SVN estimation adapted to magnitude images

According to Eqs. 1–5, local noise mask would be underestimated by the local variance of magnitude image values in low SNR regions. To avoid biased results, we used fixed point formula proposed in [18]. Based on the first two moments of Rician distribution, we evaluated the correction factor ξ as:

$$\xi(\theta_i) = 2 + \theta_i^2 - \frac{\pi}{8} \times \exp\left(\frac{\theta_i^2}{2}\right) \times \left(\left(2+\theta_i^2\right) I_0\left(\frac{\theta_i^2}{4}\right) + \theta_i^2 I_1\left(\frac{\theta_i^2}{4}\right)\right)^2, \quad (12)$$

where θ_i represents the local SNR and I_n is the n^{th} order Bessel function of first kind. Then, local noise variance σ_i^2 was computed as:

$$\sigma_i^2 = \frac{\hat{\sigma_i}^2}{\xi(\theta_i)}, \quad (13)$$

where $\hat{\sigma}_i^2$ represents biased local variance.

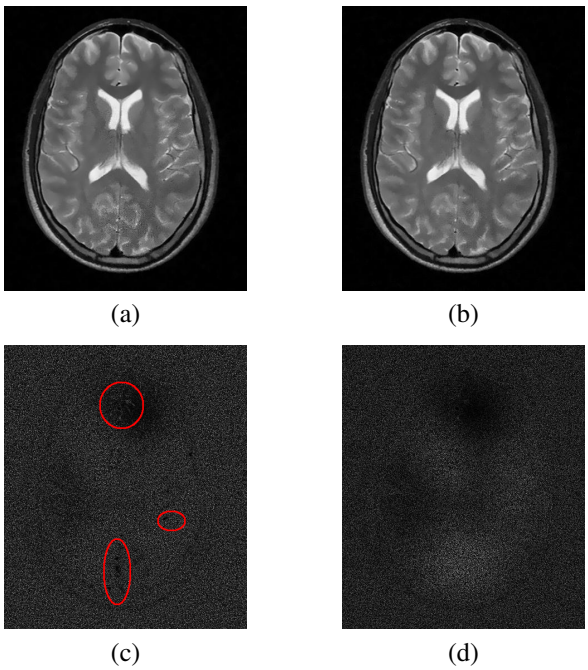

Fig. 2. Denoising results on corrupted image (average 10% non-uniform noise) with standard NLM (a) and NLM with SVN mask (b). PSNRs are 33.4162 and 34.7183 for NLM and SNV-NLM, respectively. Absolute values of residual images (enhanced by a factor 10) are shown in (c) and (d); the red ellipses highlight the image structures lost by standard NLM.

4. RESULTS

In order to evaluate the performances of NLM filter with our SVN mask (hereafter SVN-NLM), we corrupted noise-free MR images with both Gaussian and Rician spatially varying noise and integrated the estimated noise mask in Eq. 11 to adapt voxel-by-voxel the filter strength as function of the local noise power. Due to high computational complexity of NLM algorithm, we used a multi-GPU implementation [19] in both pre-processing (standard NLM) and denoising (SVN-NLM) steps. Visual inspection and residuals between noisy

and denoised image have been used to rate the quality of denoising. As quality measure we evaluated Peak SNR (PSNR):

$$\text{PSNR}(\hat{f}(x), f(x)) = 10 \log_{10} \frac{M^2}{\frac{1}{|\Omega|} \sum_{x \in \Omega} (f(x) - \hat{f}(x))^2}, \quad (14)$$

where M is maximum value of noise-free image ($f(x)$) and $\hat{f}(x)$ is the denoised image.

SVN-NLM-denoised and residual images (Fig. 2(b)-(d)) show high performance denoising without sensible removal of image structures. Compared with standard NLM, our method produces better results in terms of both visual inspection and PSNR, with a gain of ~ 1.3 dB (Fig. 2).

Moreover, to confirm the stability of our noise estimation scheme, we corrupted the ground truth with uniform noise. As shown in Fig. 3, SVN-NLM produces similar results in comparison with standard NLM.

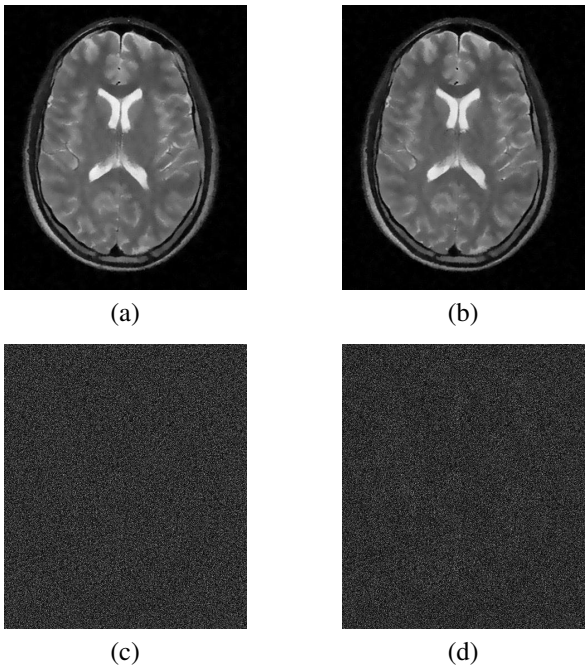

Fig. 3. Denoising results on corrupted image (10% uniform noise) with standard NLM (a) and NLM with SVN mask (b). 31.1033 and 31.1071 are PSNRs for NLM and SNV-NLM, respectively. Absolute values of residual images (enhanced by a factor 10) are shown in (c) and (d).

Finally, we compared our method with an implementation of the state-of-the-art NLM algorithm for pMRI, proposed by [13]. The different strategies to estimate the only-noise image and to statistically handle the patch-related effects of the noise variance strongly influence denoising results in case of non-uniform noise distribution. In this context, our method outperforms previous noise estimation and, accordingly, denoising in terms of both structure preservation and PSNR, with a gain of ~ 0.8 dB (see Fig. 4).

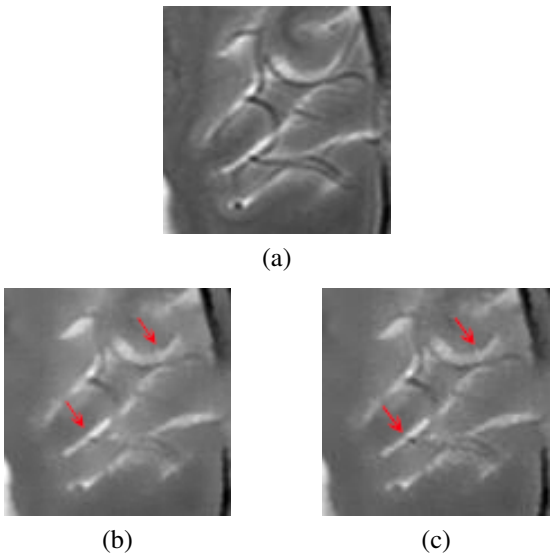

Fig. 4. Denoising results on "ground truth" (a) corrupted with an average 10% non-uniform noise. PSNRs of NLM proposed in [13] (b) and our SVN-NLM (c) are 33.9606 and 34.7305, respectively. Red arrows highlight most relevant differences between images.

5. DISCUSSION

In this study, a new method for MRI noise estimation has been presented to address the problem of biased estimation in case of spatially dependent noise distribution when background-based variance extraction is performed. Visual inspection clearly proves better results compared to standard NLM filter where anatomical structures are visible in image residuals. Moreover, both quality measure and PSNR demonstrate the ability of SVN-NLM to remove noise adaptively according to local noise variance. As our SVN estimation does not need an *a priori* knowledge of sensitivity maps and subsampling factor, the derived noise mask is applicable on parallel MR images reconstructed with both SENSE and GRAPPA techniques. Moreover, our SVN estimation outperforms previous noise calculation in case of non-uniform noise distribution [13, 14, 15]. In particular, compared to denoising method proposed in [13], we obtain both better PSNR results and gain in contrast-to-noise ratio (CNR).

On the other hand, as our approach has been demonstrated to produce similar results as the standard NLM in case of uniform noise distribution, SVN-NLM is robust enough to be applicable also on general MRI datasets (both sMRI and pMRI).

In conclusion, the application of our method in post-processing tasks of both standard and parallel MRI can clearly benefit not only visual inspection, but also quantitative techniques that rely on good quality of the data.

6. REFERENCES

[1] Hákon Gudbjartsson and Samuel Patz, "The rician distribution of noisy mri data," *Magnetic Resonance in Medicine*, vol. 34, no. 6, pp. 910–914, 1995.

[2] Jan Sijbers, Dirk Poot, Arnold J den Dekker, and Wouter Pintjens, "Automatic estimation of the noise variance from the histogram of a magnetic resonance image," *Physics in medicine and biology*, vol. 52, no. 5, pp. 1335, 2007.

[3] Olaf Dietrich, José G Raya, Scott B Reeder, Michael Ingrisch, Maximilian F Reiser, and Stefan O Schoenberg, "Influence of multichannel combination, parallel imaging and other reconstruction techniques on mri noise characteristics," *Magnetic resonance imaging*, vol. 26, no. 6, pp. 754–762, 2008.

[4] Santiago Aja-Fernández, Antonio Tristán-Vega, and Carlos Alberola-López, "Noise estimation in single-and multiple-coil magnetic resonance data based on statistical models," *Magnetic resonance imaging*, vol. 27, no. 10, pp. 1397–1409, 2009.

[5] Anagha Deshmane, Vikas Gulani, Mark A Griswold, and Nicole Seiberlich, "Parallel mr imaging," *Journal of Magnetic Resonance Imaging*, vol. 36, no. 1, pp. 55–72, 2012.

[6] James F Glockner, Houchun H Hu, David W Stanley, Lisa Angelos, and Kevin King, "Parallel mr imaging: A users guide1," *Radiographics*, vol. 25, no. 5, pp. 1279–1297, 2005.

[7] Klaas P Pruessmann, "Encoding and reconstruction in parallel mri," *NMR in Biomedicine*, vol. 19, no. 3, pp. 288–299, 2006.

[8] Mark A Griswold, Peter M Jakob, Robin M Heidemann, Mathias Nittka, Vladimir Jellus, Jianmin Wang, Berthold Kiefer, and Axel Haase, "Generalized autocalibrating partially parallel acquisitions (grappa)," *Magnetic Resonance in Medicine*, vol. 47, no. 6, pp. 1202–1210, 2002.

[9] Klaas P Pruessmann, Markus Weiger, Markus B Scheidegger, Peter Boesiger, et al., "Sense: sensitivity encoding for fast mri," *Magnetic resonance in medicine*, vol. 42, no. 5, pp. 952–962, 1999.

[10] Santiago Aja-Fernández, Gonzalo Vegas-Sánchez-Ferrero, and Antonio Tristán-Vega, "About the background distribution in mr data: a local variance study," *Magnetic Resonance Imaging*, vol. 28, no. 5, pp. 739–752, 2010.

[11] Antoni Buades, Bartomeu Coll, and Jean-Michel Morel, "A review of image denoising algorithms, with a new one," *Multiscale Modeling & Simulation*, vol. 4, no. 2, pp. 490–530, 2005.

[12] Pierrick Coupé, Pierre Yger, Sylvain Prima, Pierre Hellier, Charles Kervrann, and Christian Barillot, "An optimized blockwise nonlocal means denoising filter for 3-d magnetic resonance images," *Medical Imaging, IEEE Transactions on*, vol. 27, no. 4, pp. 425–441, 2008.

[13] José V Manjón, Pierrick Coupé, Luis Martí-Bonmatí, D Louis Collins, and Montserrat Robles, "Adaptive nonlocal means denoising of mr images with spatially varying noise levels," *Journal of Magnetic Resonance Imaging*, vol. 31, no. 1, pp. 192–203, 2010.

[14] O Dietrich, J G Raya, M Ingrisch, M F Reiser, and O Schoenberg, "Noise characteristics in mri with multichannel arrays, parallel imaging, and reconstruction filters," *in Proc. International Society of Magnetic Resonance in Medicine*, 2007.

[15] Jelle Veraart, Jeny Rajan, Ronald Peeters, Alexander Leemans, Stefan Sunaert, and Jan Sijbers, "Estimation of spatially variable rician noise map in diffusion mri," *in Proc. International Society of Magnetic Resonance in Medicine*, 2013.

[16] Santiago Aja-Fernández, Antonio Tristán-Vega, and W Scott Hoge, "Statistical noise analysis in grappa using a parametrized noncentral chi approximation model," *Magnetic Resonance in Medicine*, vol. 65, no. 4, pp. 1195–1206, 2011.

[17] Santiago Aja-Fernández, Gonzalo Vegas-Sánchez-Ferrero, and Antonio Tristán-Vega, "Statistical noise analysis in sense parallel mri," .

[18] Cheng Guan Koay and Peter Basser, "Analytically exact correction scheme for signal extraction from noisy magnitude mr signals," *Journal of Magnetic Resonance*, vol. 179, pp. 317–322, 2006.

[19] Giuseppe Palma, Francesco Piccialli, Marco Comerci, Pasquale De Michele, Pasquale Borrelli, Salvatore Cuomo, and Bruno Alfano, "3d non-local means denoising via multi-gpu," *Proceedings of the 2013 Federated Conference on Computer Science and Information Systems*, pp. 495–498, 2013.